Refinement of Glider Aerodynamic Design using CFD

Johannes J. Bosman
School of Mechanical and Nuclear Engineering
North-West Universty
Potschefstroom 2520, South Africa
johan.bosman@nwu.ac.za

Abstract

Only small aerodynamic improvements are possible on current sailplane designs when using current design and analysis methods. In order to obtain a substantial improvement in cross-country performance, areas which are not fully optimized must receive attention. These areas include regions where complex flows exist on the surface and special analysis tools are required. New developments in CFD laminar to turbulent transition modeling allow optimization of complex 3-D flow areas such as the wing-fuselage junction. To demonstrate the overall effect of using CFD to optimize many small areas around the sailplane, the total performance improvement was compared against a baseline sailplane. The possible performance improvement for an 18m Class sailplane was calculated and found to be around 3 glide-ratio points.

Introduction

Many designers and researchers have speculated that without features such as boundary layer suction, it is difficult to improve the aerodynamic performance of current sailplanes. The question then becomes whether new sailplane models could have significant performance gains over older designs, without such features.

For a sailplane manufacturing company, if only aerodynamic performance is considered, an improvement of at least 2 glide-ratio points is necessary before the effort can be made to introduce a new model. When comparing today's top performing 18m racers (best L/D of around 53:1), this relates to a best L/D of around 55:1. In order to obtain this performance increase, assuming a 600 kg glider flying at 110 km/h, the following drag reduction needs to be achieved:

$$\begin{array}{lll}
\text{Drag}_{\text{current}} = & (600\,\text{kg}/53) \times (9.81\text{m/s}^2) & = 111\text{ N} \\
\text{Drag}_{\text{new}} = & (600\,\text{kg}/55) \times (9.81\text{m/s}^2) & = 107\text{ N} \\
\text{Drag difference} = & & 4\text{ N}
\end{array}$$

To put this 4 Newton drag value into perspective, the drag of an average-sized human hand with the palm perpendicular to the air flow direction at 110 km/h is around four times this value at 16 N! At higher speeds, around 200 km/h, the drag reduction required is around 9 N if a 2-point glide-ratio improvement is also assumed.

Before looking at achievable ways to obtain such a seemingly small improvement, part of the current design procedure for high performance sailplanes will be briefly discussed.

Presented at the XXXI OSTIV Congress, 8–15 August 2012, Uvalde TX USA

Aerodynamic Design Procedure

There are two somewhat conflicting aerodynamic requirements for a high performance sailplane. First, the aircraft needs to have high performance during the cruise phase, which mostly relates to the minimum drag of the main wing airfoil and the total wetted area of the sailplane.

The second requirement is to have high performance while in the climb configuration, which mostly relates to the maximum lift coefficient of the airfoil and an optimized wing planform for minimum induced-drag.

In the past, numerical approaches such as panel codes have been used for the design of airfoils in order to reach these objectives of low drag and high lift. In the case of the JS-1 sailplane, XFOIL [1] was used for the airfoil design. The result was a thin 12.7% thick airfoil (Fig. 1) that provided good high speed performance. KKAERO [2] was then used for the 3-D wing design, winglet design, and optimization of the planform. The airfoil drag characteristics at various Reynolds numbers were also included in the optimization of the aspect ratio and planform.

In the region of the wing-fuselage junction, a combination of the design codes XFOIL and KKAERO were used to design the root profile, which showed less drag in turbulent flow than an airfoil designed for laminar flow. The angle-of-attack at the root section was also increased to compensate for lift loss due to the

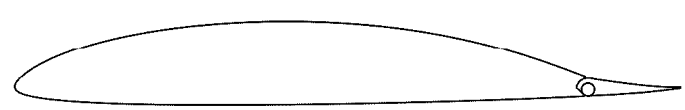

Figure 1: Main wing profile (T12) for the JS-1 sailplane

presence of the fuselage. This feature improved the spanwise load distribution required to be close to elliptical for minimum induced drag. Further changes to the root profile were made to ensure a moderate adverse pressure gradient that would reduce separation problems on the upper root surface.

For the aerodynamic design of the wing for the JS-1, the procedure followed was nothing new at the time. A competitive glide ratio of 53:1 was, however, obtained as a result of using such a thin airfoil and making it work structurally.

Designers now find themselves at a point where it is very tricky to improve on the current laminar profiles. Further improvements of the planform and aspect ratio are also unlikely due to the limitations on span and stall speeds. In order to extract additional cross-country performance from an 18m-Class sailplane, areas which have not yet been fully optimized must be given attention. Generally speaking, these are regions where complex surface flows exist, but they require special analysis tools.

Complex 3-D Flow Areas

The regions on a sailplane where complex 3-D flow phenomena occur are areas such as:

- wing-fuselage junction
- winglets
- fin-fuselage and fin-tailplane junctions
- control horn fairings
- wing tip wheels / skids and tail wheel
- internal cockpit ventilation

In most of these cases, interference drag is the result whenever two or more aerodynamic bodies are combined. Due to the inherent difficulty of applying theoretical or analytical methods to calculate and compare the interference drag in these areas, most prior research has thus been limited to experimental approaches. However, there are now refinements in computer analysis tools that permit further investigation into these challenging flow regions.

Requirements for Analysis of Complex 3-D Flow Areas

Sailplanes operate in a speed range where both laminar and turbulent flow regions exist on the surface. The instability of laminar flow and the transition to turbulence have always been a subject of great interest in fluid mechanics. The reason for this is that the prediction of transition from laminar to turbulent flow is important in the accurate calculation of aerodynamic parameters such as drag, lift, pitching moments, and even heat transfer. Skin friction is dramatically higher in turbulent boundary layers than it is in laminar regions. It is thus essential to be able to predict the exact location of transition on a surface, and this explains why a large amount of experimental, theoretical, and numerical work has been done over the last decade.

Computational Fluid Dynamics (CFD)

Since the completion of the design of the JS-1 sailplane, the field of Computational Fluid Dynamics (CFD) has grown considerably. Much work has been done on laminar-to-turbulent transition prediction models within CFD - which is the main concern when accurate drag and lift predictions must be made, during the design of sailplanes.

Boundary-layer transition on the surface of a sailplane is the result of a sequence of complex flow phenomena. In the first stage of the transition process, the ambient disturbances such as noise, vibrations, and free-stream turbulence influence the laminar boundary layer. This is called the boundary layer receptivity. From there the small disturbances are responsible for the initial conditions that influence the development of the complex mechanisms which will lead to turbulence. All of these flow characteristics must be modelled accurately for the correct prediction of the transition location.

The following CFD transition capable approaches are available:

- Direct Numerical Simulation (DNS)
- Large Eddy Simulation (LES)
- Reynolds Averaged Navier-Stokes (RANS)

The RANS method applied to the aerodynamic analysis of flows around sailplanes proves to be the most feasible for currently available computer resources. The model used in this research is the model by Walters and Leylek [3] which is available in ANSYS FLUENT®.

Other variations within the RANS methods are also used to properly model the flow characteristics, but it is beyond the scope of this article to compare different transition models.

For each simulation, a computational flow domain (flow volume surrounding the aircraft) is created in a CAD environment similar to the flow domain shown in Fig. 2. A typical flow domain has boundary conditions such as inlets, outlets, symmetry walls, and also the geometry of the sailplane. This computational domain is then divided (meshed) into small segments throughout the entire domain. In areas where more detail of the

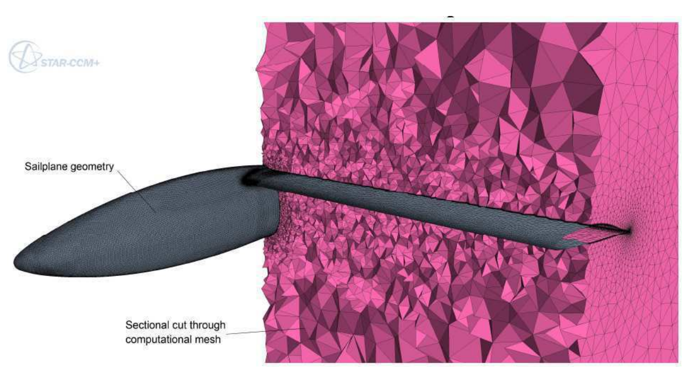

Figure 2: Computational flow domain

flow behavior is required, the mesh is refined in order to capture the activity. The higher the number of cells in the computational mesh, the more computer-intensive the simulation becomes and the longer it takes to obtain a solution.

For reference, simulations for the improvement of the JS-1 sailplane have been solved on a High Performance Computer cluster (HPC) at North-West University. The average sized computational mesh contained around 35 million cells. In order to obtain a converged solution, the solver needed around 3500 iterations which typically took around 10 hours.

Analyses of Glider Geometries with CFD

Using the RANS CFD transition model is by no means perfect, and absolute drag values are certainly not obtained. However, the main advantage is comparative tests where relative drag and lift values of various geometries can be compared in a short period of time [4]. Wind-tunnel experiments and in-flight testing yield limited insight, especially for complex 3-D flow areas, whereas the use of CFD allows the researcher to analyze the combination or overall aerodynamic effect of modifications and compare results with a baseline case. The practical objective is to explore new aerodynamic improvement possibilities with CFD and to determine the feasibility for such geometric modifications.

Analysis of the Wing-Fuselage Junction

The design of the wing-fuselage intersection has long been like a stepchild to sailplane aerodynamicists. Designers were aware of the interference effects, but lacked the necessary knowledge of the complex physical flow phenomena that reside in the junction area. It has therefore been common practice to design wing-fuselage junctions by applying "rule-of-thumb" techniques rather than properly validated engineering design methods.

The fuselage and wing must be designed to operate at a wide angle-of-attack range, especially for un-flapped (Standard Class) sailplanes. Significant separation problems may occur at high angles-of-attack due to the super-position of adverse pressure gradients from the fuselage and wing. Further complications arise from the alpha-flow [5], as illustrated by Fig. 3. In this case, the acceleration of flow around the fuselage at high angles-of-attack increases the inflow angle at the root even further.

CFD now allows more accurate analysis of the flow in this region of the sailplane, and a few configurations that have been simulated regarding the wing-fuselage junction are discussed next.

High-Wing Configuration

It is beneficial to compensate for lift loss due to the presence of the fuselage by increasing the incidence of the root profile. It might in fact seem that the alpha-flow effect is automatically compensating for the lift loss. However, the alpha-flow effect actually makes it difficult to optimize the wing lift towards an elliptical load distribution for the wide range of operating angles-of-attack experienced by a sailplane.

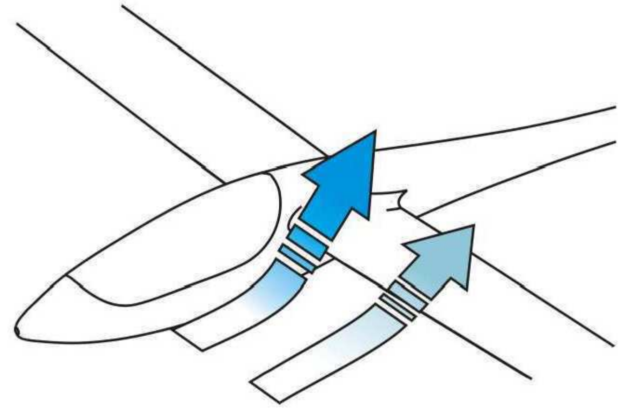

Figure 3: Alpha-flow effect increase in angle-of-attack as seen by the root sections

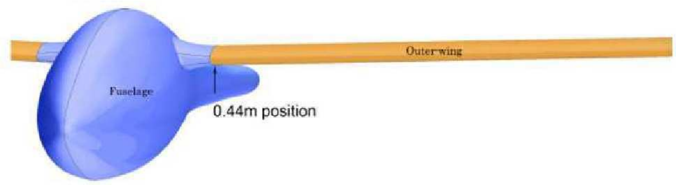

(a) Mid-wing Baseline geometry

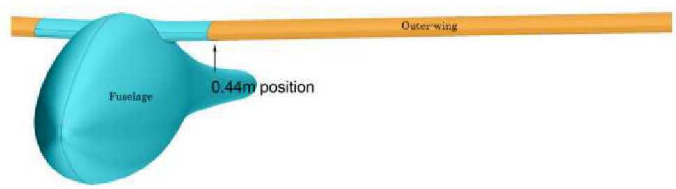

Figure 4: Baseline wing position (a) and high-wing configuration (b)

The technique then is to first minimize the alpha-flow effect and only then optimize the circulation for minimum induced drag. In order to minimize the alpha-flow effect, the wing can be shifted higher relative to the fuselage. For this particular comparison, the high-wing configuration was simulated and compared with the baseline (mid-wing) configuration as shown in Fig. 4. No modifications were made to the wing twist distribution, root airfoils, or planform. The root section of the baseline wing was used and moved as high on the fuselage as practical. It can be seen from Fig. 4 that a little more wing area is introduced because of the fuselage curvature when the wing is moved higher. The distance from the center line, from where the outer wing section starts, was kept the same for adequate comparison with the baseline case. No geometric optimization was done (such as larger fillets around the junction or airfoil changes).

In most of these simulations, the fuselage and stub-wing section shown in both cases in Fig. 4 were used in the calculation of drag and lift and then compared with other configurations. The outer wing section was kept the same.

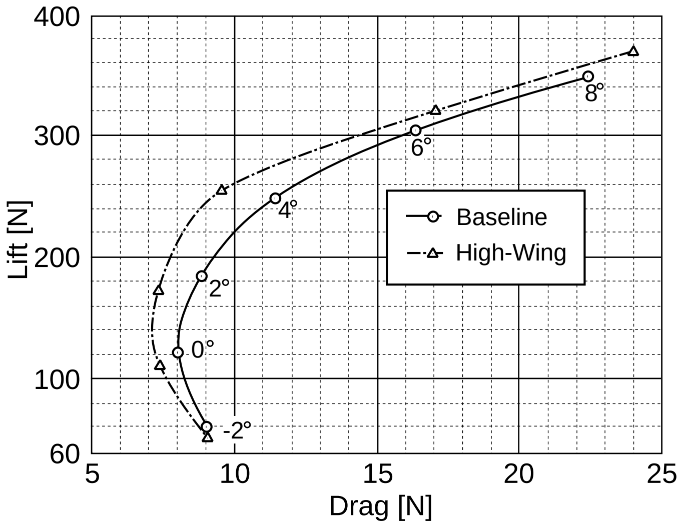

Figure 5: Performance polar comparison between baseline and high-wing configuration (at 125 km/h)

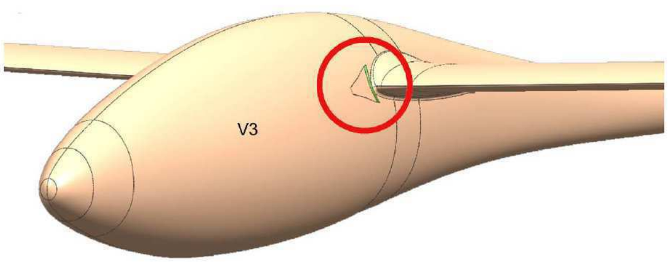

Figure 6: Root suction device (NWU Patent)

Figure 5 shows the results of the high-wing configuration compared with the baseline (mid-wing) configuration. Not only is it minimizing the alpha-flow effect, it also shows considerably less drag than the mid-wing configuration. The lift and drag values shown in the figure are thus calculated for the fuselage and stub-wing section only. Also, the figures are only for half a sailplane, due to the fact that half of the geometry is simulated (the CFD model takes advantage of symmetry to reduce the solution time). Thus the drag difference must be multiplied by two. A relative drag reduction of between 3 and 4 N was obtained with the high-wing configuration over the baseline.

Root Suction Device

Another promising aerodynamic feature is the root suction device (patented by North-West University). The root suction device (Fig. 6) combines two principles. First, it has been shown that suction through a slot is able to remove the low energy layer in the boundary layer and prevent transition to turbulent flow. The energized boundary layer can then move further along the surface against an adverse pressure gradient before the transition to turbulent flow occurs. Flow separation may also be prevented. Second, the stagnation point on a bluff body is effectively de-

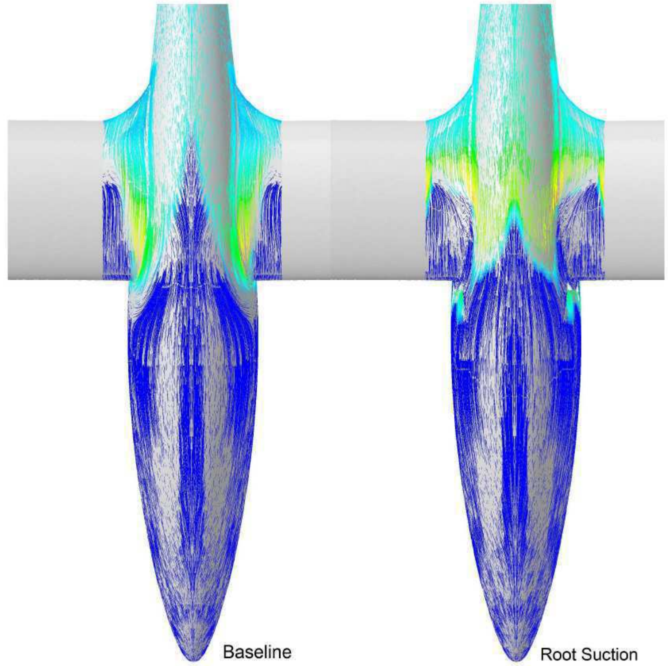

Figure 7: Top view of the turbulence intensity flowlines for the baseline and root suction system cases

pressurized. Drag can significantly be reduced by channeling the high pressure from the stagnation point at the leading edge and into the wake by means of a bypass channel. Drag reductions in the order of 50% have been measured in a wind tunnel on a sphere with a hole through the middle [6].

The root junction benefits from the suction device in several ways. Excess air particles are channelled away from the stagnation point at the wing root leading edge. The root area is thus de-pressurized and the low energy boundary layer is relieved from the adverse pressure gradient. In this case, the low energy boundary layer is also removed and laminar flow is encouraged on the side of the fuselage and bottom surfaces of the wing. If laminar flow is present on the wing surface close to the fuselage, a laminar flow airfoil can also be used, which can produce significantly less drag than a turbulent airfoil.

If flow separation due to the adverse pressure gradient is avoided, the vortex strength can be reduced and a considerable amount of interference drag can also be avoided.

Figure 7 shows the CFD results and indicates the difference in the amount of laminar flow for the two configurations. There is a significant improvement in the amount of laminar flow on the wing root surfaces and on the side of the fuselage. The turbulent wedge on the wing roots which is seen in the baseline case is largely eliminated. The CFD-determined maximum drag reduction is around 0.6 N for the incorporation of the root suction system.

This reduction in drag is mainly as a result of viscous drag that is reduced. Also seen in this case is a small reduction in

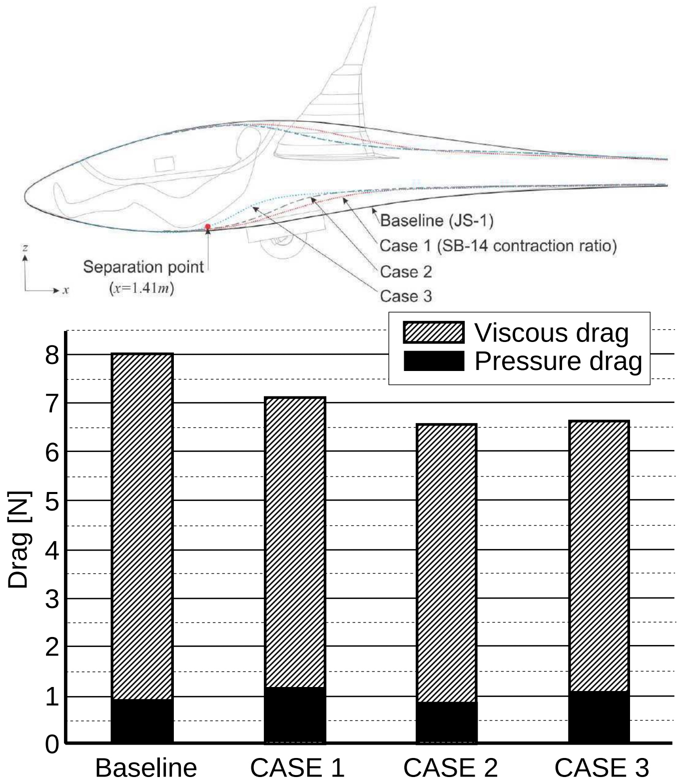

Figure 8: Drag comparison results for the different contraction ratio cases

pressure drag, which relates to interference drag that is saved.

Fuselage Shape and Contraction Ratio

The contraction ratio of the fuselage behind the cockpit area can have a large effect on drag. This is due to the reduction of surface area with an increase in the contraction ratio. At some point, however, separation of the boundary layer may occur if the adverse pressure gradient is too steep due to a large contracted geometry. The optimum contraction ratio of the fuselage can be found by means of wind-tunnel experiments, but these are costly and time-consuming.

A simple case study was therefore made with the use of CFD to determine the optimum contraction ratio at a flight speed of 125 km/h.

Figure 8 shows the reduction in drag that can be obtained when the contraction ratio of the fuselage is dramatically changed without changing the cockpit area.

An optimum ratio exists for this flight speed in this case, and more aggressive contractions will have increased drag due to flow separation. The separation point is also shown in Fig. 8 in the excessive contraction ratio case 3. The CFD analysis indicates that a moderate contraction ratio can yield a drag reduction of up to 2.5 N.

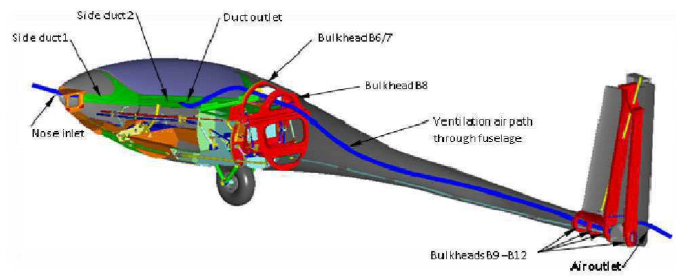

Figure 9: Typical ventilation path through a sailplane

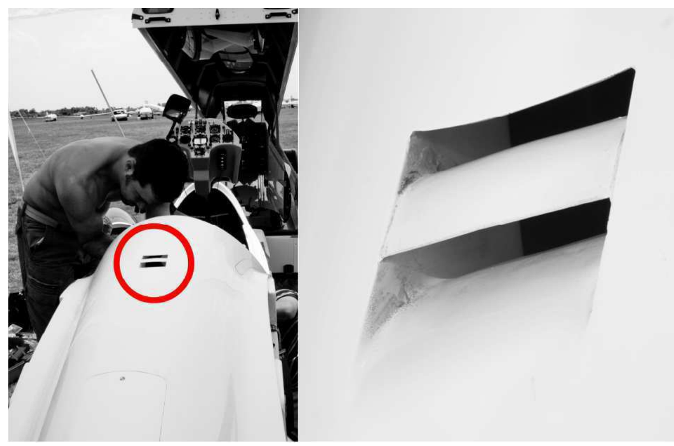

Figure 10: JS louvered air extractor

Cockpit Ventilation

In order to have proper cockpit ventilation, the air must have an efficient way of exiting the aircraft. A typical internal ventilation path (Fig. 9) has many restrictions that cause internal drag. A louvered air extractor (Fig. 10) has been designed for minimum disturbance of the external boundary layer when air is exiting the fuselage. It is also positioned where the external static pressure is at a minimum. This feature lowers the internal ventilation drag over conventional systems. CFD was then used to calculate the reduction in drag by using such a system over conventional systems. CFD calculations show a 0.3 N total drag reduction.

Control Horn Fairings

With an air extractor installed, there is no longer any need for an internal ventilation exit at the rudder control horns, so rudder horn fairings can be considered for a reduction in drag. CFD has been used to optimize the fairing shape as shown in Fig. 11, giving a calculated 0.4 N reduction in overall drag.

Performance of the Next Generation 18m Sailplane

Several of the features discussed above are relatively simple to implement, but others such as the high-wing configuration require significant changes in the geometry. However, with the

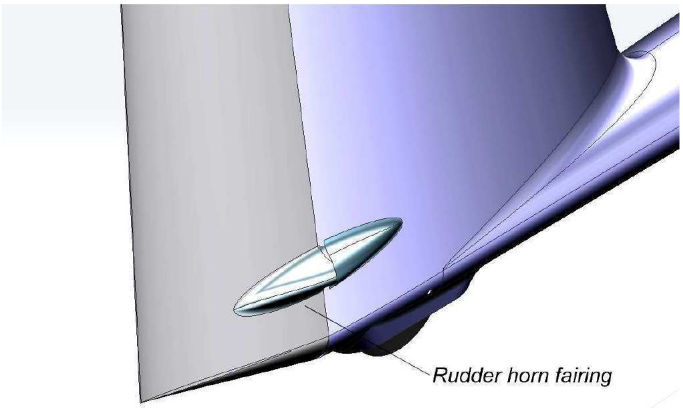

Figure 11: Implementation of rudder horn fairings on the JS1 Revelation

Table 1: Summation of the drag reduction features

High Wing Configuration	3.0 N
Root Suction	0.6 N
Fuselage Shape	2.5 N
Cockpit Ventilation	0.3 N
Control Horn Fairings	0.4 N
Fin-Fuselage Junction	0.5 N
Total Drag Reduction	7.3 N

latest CFD capability, the next generation sailplane can become a reality — and with this example set of drag reduction features, the overall drag reduction can be summed to be 7.3 N as shown in Table 1. A typical 18m-sailplane could then theoretically achieve a glide ratio of 56:1 or more!

References

[1] Drela, M. and Giles, M. B., "Viscous-Inviscid Analysis of Transonic and Low Reynolds Number Airfoils," *AIAA Journal*, Vol. 25, No. 10, 1987, pp. 1347–1355.

[2] Kubrynski, K., "Application of the panel method to subsonic aerodynamic design," *Inverse Problems in Engineering*, Vol. 5, No. 2, 1997, pp. 87–112.

[3] Walters, D. K. and Leylek, J. H., "Computational Fluid Dynamics Study of Wake-induced Transition on a Compressor-like Flat Plate," *Journal of Turbomachinery*, Vol. 127, No. 1, 2005, pp. 52–63.

[4] Bosman, J. J., *Evaluation of new aerodynamic concepts using CFD for the improvement of a glider fuselage*, Ph.D. thesis, School for Mechanical and Nuclear Engineering of the North- West University, Potchefstroom Campus, Potchefstroom, South- Africa, 2012.

[5] Boermans, L. M. M. and Terleth, D. C., "Wind tunnel tests of eight wing-fuselage combinations," *OSTIV Publication XVII — Proceedings of the XVIII OSTIV Congress*, OSTIV, Hobbs, New Mexico, 1983, pp. 10–25.

[6] Grosche, F. R. and Meier, G. E. A., "Research at DRL Göttingen of bluff body aerodynamics, drag reduction by wake ventilation and active flow control," *Journal of Wind Engineering and Industrial Aerodynamics*, Vol. 89, December 2001, pp. 1201–1218.